Thermoelastic Properties of Plain Weave Composites for Multilayer Circuit Board Applications

Eric N. Brown and N.R. Sottos

Department of Theoretical and Applied Mechanics
University of Illinois at Urbana-Champaign
Urbana, IL 61801

Summary

The thermoelastic properties of several common woven glass/epoxy substrate materials were characterized in both the warp and fill directions. Five common commercially pressed cores (1080, 2116, 2313, 3313, 7628) were obtained from Polyclad, Inc. The cores consisted of either one or two plies of C-staged woven glass epoxy substrate sandwiched between 1 ounce copper cladding. After the copper was removed from the cores, samples were cut for either mechanical property characterization or microstructural analysis with the test axis lying along either the warp or fill direction. The crimp angle and relative fiber volume fraction of each fabric was first determined from photomicrographs of polished cross-sections. Next, Young's modulus was measured via standard tension tests at room temperature. The storage and loss moduli were then measured as function of temperature using dynamic mechanical analysis (DMA). Finally, the coefficients of thermal expansion were determined using constant force thermal mechanical analysis (TMA) measurements. All of the substrates showed significant differences in microstructure and material properties between the warp and fill directions. Most of the laminates had a much lower crimp angle in the warp direction, which resulted in a higher modulus and lower coefficient of thermal expansion than the fill direction. Of the cores investigated, the properties of 3313 were the most balanced.

1. INTRODUCTION

Woven glass fabric/epoxy composites are used extensively as substrate materials for multilayer printed circuit boards. The boards are fabricated by consolidating layers of copper and glass/epoxy prepreg in a press under a prescribed temperature and pressure cycle. Significant residual stresses develop during the manufacturing process of these laminated structures, which can lead to unacceptable warpage of the board. In order to predict the warpage of the boards either by classical lamination theory or finite element analysis, the elastic properties of the constitutive materials must be known.

Many different plain weave fabric styles are currently used in multilayer circuit boards. The fabrics are often unbalanced, having different numbers of fiber bundles or different size fiber diameters in the warp and fill directions. Due to the variation in the fiber bundle sizes, the crimp of the fiber bundles is often unbalanced and depends on the fabric styles. Hence, different fabrics can have very different properties. In general, the properties of the woven glass/epoxy substrates used in multilayer boards have not been characterized or are not well documented.

In the current investigation, the thermoelastic properties of several common woven glass/epoxy substrate materials (1080, 2116, 2313, 3313, 7628) are studied. The elastic modulus and coefficient of thermal expansion (CTE) are measured in both the warp and fill directions of the composite. In addition, the glass transition temperature and temperature dependent moduli are also determined. Properties are correlated with the fabric microstructure (weave parameters).

2. MATERIALS

Five common commercially pressed cores were obtained from Polyclad, Inc. The cores consisted of either one or two plies of C-staged woven glass epoxy substrate sandwiched between 1 ounce copper cladding. Table 1 lists the fabric style of composite substrate used in each of the different cores along with the number of plies. The copper cladding was removed from the substrates using a dilute nitric acid solution. Test samples for either mechanical property characterization or microstructural analysis were then cut from the substrates.

Table 1. Woven fabric styles investigated.

	Plies per Board	Nominal Board Thickness (mm)
1080	2	0.106
2116	2	0.188
2313	2	0.168
3313	2	0.160
7628	1	0.173

3. CHARACTERIZATION OF THE WEAVE GEOMETRY

The glass/epoxy substrates in Table 1 are plain weave composites consisting of two sets of orthogonal fiber bundles. The initial set of parallel fiber bundles is defined as the warp bundles. A second set of fibers is then woven through the first and is denoted as the fill bundles. Changes in the tension and spacing of these bundles during weaving result in varying degrees of crimp. A schematic of the unit cell for the plain weave fabric is shown in Fig. 1. Since the composite properties are highly influenced by the weave geometry, the bundle sizes, crimp and fiber volume fraction must be known in both the warp and fill directions.

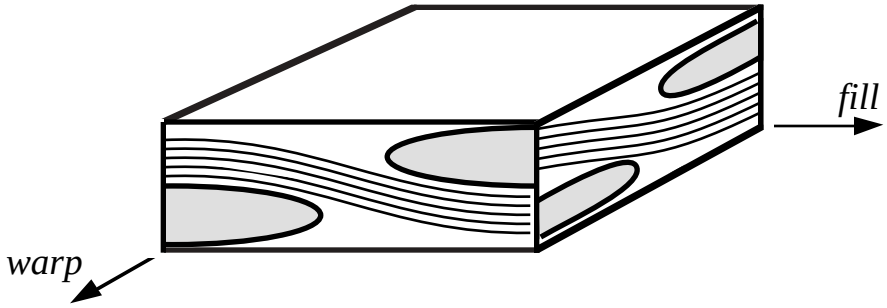

Fig. 1. Schematic of plain weave unit cell geometry.

The manufacturer provides some standard geometric specifications for each weave including the number of glass bundles per 50 mm (known as the count), the diameter of the individual fibers in the bundles and the linear density of the fabric in the warp and fill directions. The specified values for each of the fabric styles are listed in Table 2. The fiber volume fraction, f, of the substrates in the warp and fill directions is related to these geometric parameters through the expression,

$$f = \frac{(count)}{(linear\ density)t\rho_g} \tag{1}$$

where t is the thickness of the laminate given in Table 1, the count and linear density of the fabric are given in Table 2, and the density of glass ρ_g is 2.59 g/cm^3. The calculated values of f using Eq. (1) are also listed in Table 3 for each fabric.

The crimp of the fabric was determined from direct observation of the substrate microstructure. Samples were cut from the laminates such that the major axis was parallel to either the warp or fill bundle directions, mounted in an epoxy molding compound, polished and viewed at with an optical microscope. Representative micrographs of the samples are shown in Figs. 2-6. The bundle spacing and bundle aspect ratios were carefully measured and the resulting crimp angle tabulated in Table 3. For all of the laminates investigated, the aspect ratio and the approximate crimp angle of the fill bundles was larger than the value measured for the warp bundles. Hence, the warp fibers remain straighter and more in-tact (less spread out). The 3313 laminate had the most balanced microstructure while 7628, 2313 and 1080 had the largest differences between warp and fill.

Table 2. Weave properties as specified by (Owens Corning, 1988).

	Count (ends/ 50mm)		Fiber diameter (microns)		Linear density (g/km)	
	warp	*fill*	*warp*	*fill*	*warp*	*fill*
1080	118	93	5	5	11	11
2116	118	114	7	7	22	22
2313	118	126	7	7	22	22
3313	118	122	6	6	16.5	16.5
7628	87	63	9	9	68	68

Table 3. Measured aspect ratio, crimp and glass fiber volume fraction.

	Aspect ratio		Crimp Angle		Volume fraction	
	warp	*fill*	*warp*	*fill*	*warp*	*fill*
1080	4.4	9.7	6.6°	13.5°	18.8	14.8
2116	4.7	5.7	8.5°	10.2°	21.4	20.7
2313	5.5	7.9	5.7°	9.6°	26.4	28.1
3313	6.4	8.1	5.9°	5.6°	20.8	21.5
7628	5.3	7.3	6.0°	9.4°	25.6	18.6

a)

b)

Fig. 2. Photomicrographs of 1080 laminate (100x) a) warp yarns parallel to the page, fill yarns perpendicular, b) fill yarns parallel to the page, warp yarns perpendicular.

a)

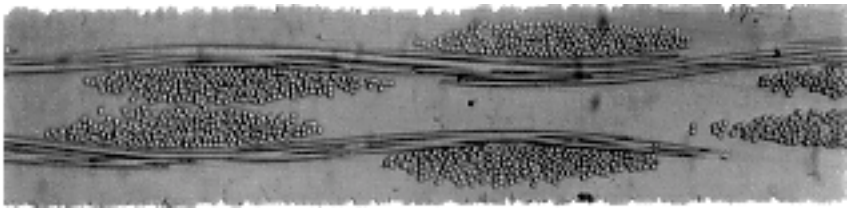

b)

Fig. 3. Photomicrographs of 2116 laminate (135x) a) warp yarns parallel to the page, fill yarns perpendicular, b) fill yarns parallel to the page, warp yarns perpendicular.

a)

b)

Fig. 4. Photomicrographs of 2313 laminate (95x) a) warp yarns parallel to the page, fill yarns perpendicular, b) fill yarns parallel to the page, warp yarns perpendicular.

a)

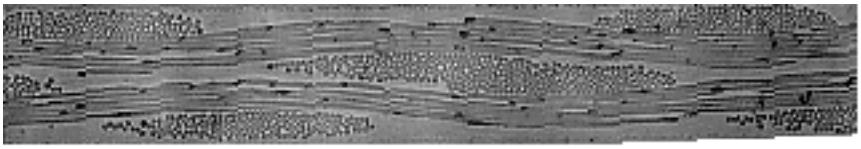

b)

Fig. 5. Photomicrographs of 3313 laminate (110x) a) warp yarns parallel to the page, fill yarns perpendicular, b) fill yarns parallel to the page, warp yarns perpendicular.

a)

b)

Fig. 6. Photomicrographs of 7628 laminate (67x) a) warp yarns parallel to the page, fill yarns perpendicular, b) fill yarns parallel to the page, warp yarns perpendicular.

4. DETERMINATION OF STORAGE AND LOSS MODULI

The elastic moduli were first measured via standard uniaxial tension tests at room temperature. Samples with a gage length of 12" and a width of 1" were cut with the testing axis along either the warp of fill directions. Five samples of each laminate type were tested and the averaged values of the Young's modulus are listed in Table 4. The storage and loss moduli of the five substrates were then measured as a function of temperature using a Perkin Elmer 7e dynamic mechanical analyzer (DMA). Smaller samples approximately 18 mm by 3.5 mm were cut in both the warp and fill directions and mounted into the DMA extension fixture as shown in Fig 7. The tests were started at -5˚C and held for a 5 minute period to allow the system and sample to stabilize. Dynamic load and displacement at a fixed frequency of 1 Hz were measured as the temperature was ramped from -5˚C to 170˚C at a rate 5˚C/min.

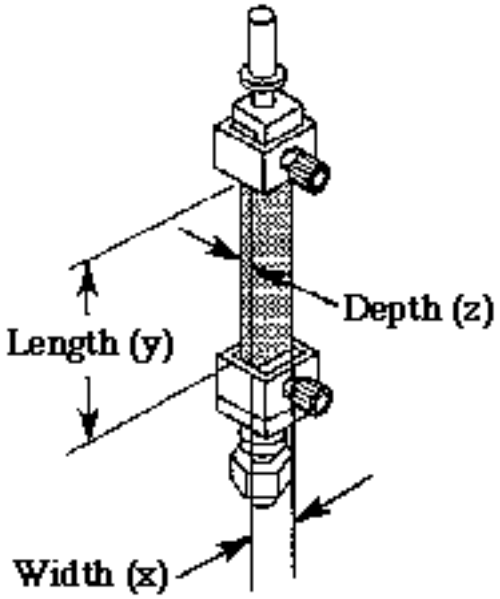

Fig. 7. Schematic of DMA extension fixture.

Representative DMA scans are shown in Fig. 8 for the 7628 substrate in the warp and fill directions. Similar modulus data is plotted for the other fabric styles in Appendix A. The loss moduli are approximately zero for all values of temperature except near the glass transition. In this region, E" peaks and the temperature measured at the maxima value of this peak is taken as the value of T_g. The measured values of T_g for each of the substrates are listed in Table 4. Variation exists in the measured T_g for the different substrates due to

differences in the epoxy matrix. All of the laminate cores were not obtained at the same time and some have a higher T_g matrix (such as the 1080) than others.

The storage moduli are nearly constant at temperatures below the glass transition temperature (T_g). Near the glass transition, the storage modulus drops off significantly. For all of the composite substrates investigated, a higher storage modulus is measured in the warp direction than the fill direction. The warp and fill relaxation behavior is also different as the fully relaxed storage modulus (above T_g) is still higher in the warp direction. The increase in stiffness is due to the smaller degree of crimp and hence straighter fibers in the warp fiber direction. In fabrics such as 1080, 2116, and 7628, the stiffness is further unbalanced due to a larger fiber volume fraction in the warp direction. Both the reduction of crimp and the increased fiber volume fraction lead to an increase in composite properties dominated by the glass. Fabrics such as 2313 and 3313 have more balanced properties due to a larger fiber volume fractions in the fill direction than the warp. Additionally, the crimp angles in the warp and fill are nearly equal for the 3313 fabric.

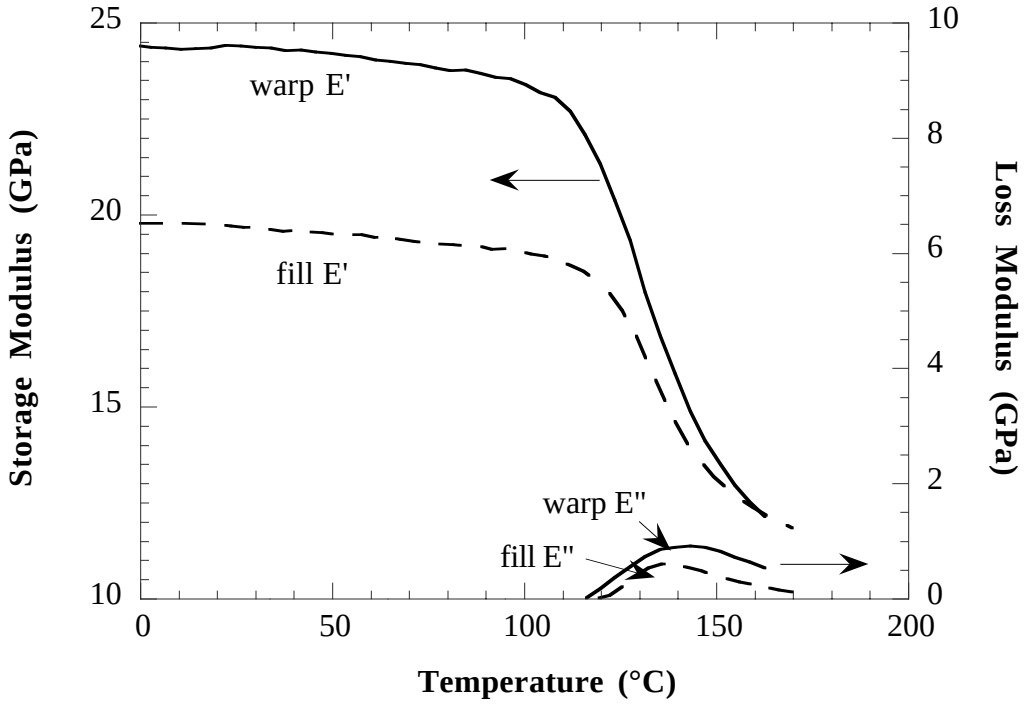

Fig. 8. Loss and storage modulus as a function of temperature for 7628 in the warp and fill directions measured using DMA.

Table 4. Room temperature modulus and glass transition temperature.

	E (GPa)		T_g (°C)	
	warp	*fill*	*warp*	*fill*
1080	18.1	12.3	166	166
2116	17.7	16.2	133	135
2313	20.8	14.1	131	131
3313	16.1	13.7	130	133
7628	24.5	19.8	138	138

5. DETERMINATION OF COEFFICIENTS OF THERMAL EXPANSION

The in-plane CTEs of the five substrates were measured below the glass transition temperature using the Perkin Elmer DMA 7e in constant force mode for thermal mechanical analysis (TMA). Rectangular samples were cut in both the warp and fill directions to measure approximately 15 mm by 3.5 mm and mounted into the TMA extension fixture as shown in Fig 9. Tests were again started at -5˚C and held for a 5 minute period to allow the system and sample to stabilize. The expansion was then measured as the temperature was ramped from -5˚C to 170˚C at a rate 5˚C/min.

Representative TMA scans are shown in Fig. 10 for the 7628 substrate in both the warp and fill directions. Similar expansion data for the other fabric styles are included in Appendix B. The expansion is linear, with a constant slope up to the onset of the glass transition at 125˚C. The glass transition is complete by 150˚C at which point, the expansion behavior changes significantly. Values of CTE below T_g were calculated in both the warp and fill directions from the slope of expansion verses temperature curves in the region from 0˚ to 100˚C and listed in Table 5. The increase in sample compliance above T_g created difficulties with the expansion fixture. As a result, CTEs were not measured above the T_g for any of the substrates.

For all of the fabric styles except 3313, the CTE is larger in the fill direction. The larger crimp angle and lower fiber volume fraction in the fill direction favors a more matrix dominated CTE. Also, the stiffness is lower in the fill direction and provides less restriction to the expansion of the matrix than encountered in the warp direction. The CTEs are nearly equal in the 3313 laminate, which has a more balanced construction.

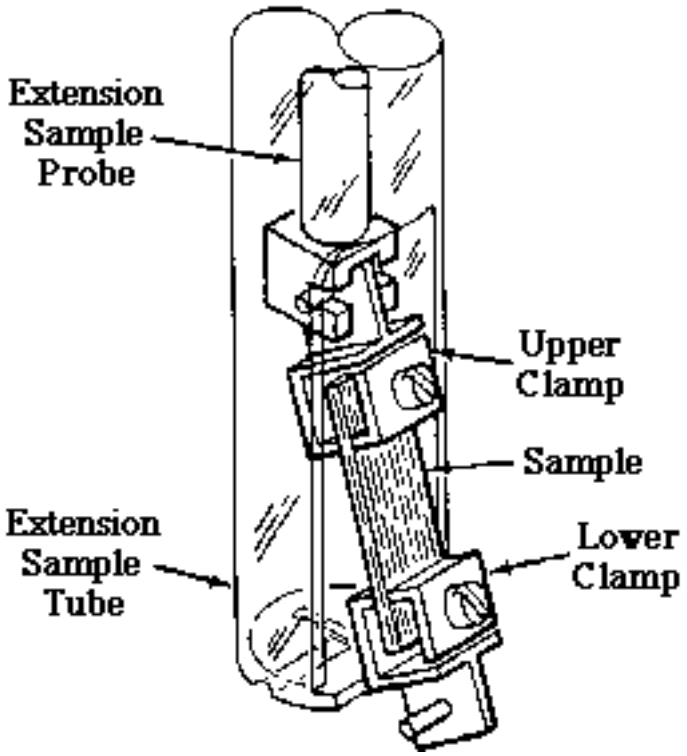

Fig. 9. Schematic of TMA extension fixture.

Table 5. Measured value of CTE below T_g for each fabric.

	Warp CTE (ppm/˚C)	Fill CTE (ppm/˚C)
1080	14.7	24.6
2116	18.0	19.3
2313	15.1	18.0
3313	15.4	14.9
7628	13.5	16.1

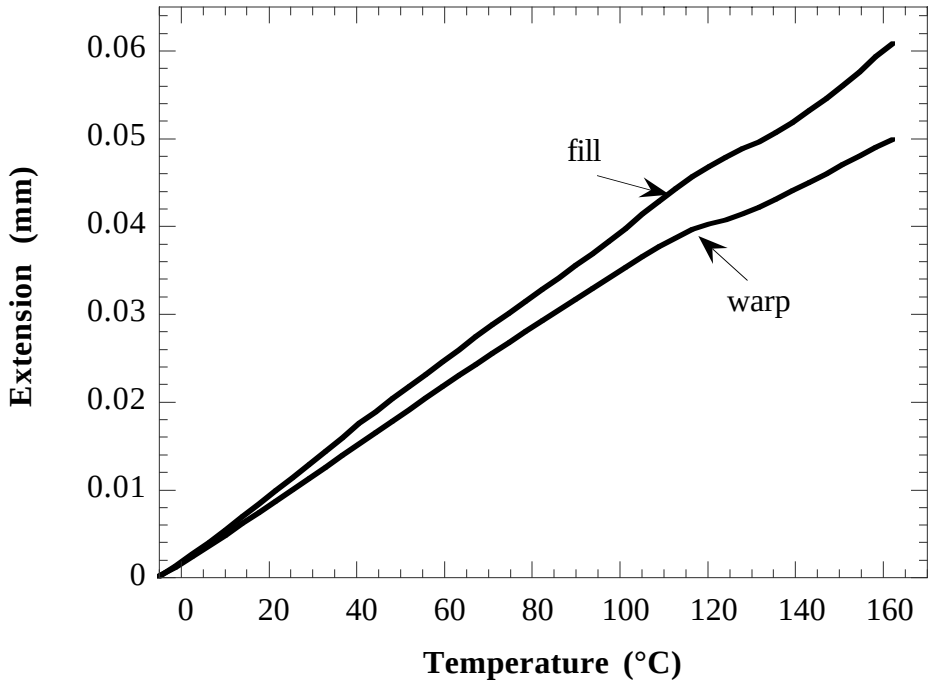

Fig. 10. Expansion as a function of temperature for 7628 in the warp and fill directions as measured by TMA.

ACKNOWLEDGMENTS

The authors gratefully acknowledge the financial support of Motorola Corporate Manufacturing Research Center (CMRC), technical support from Andrew Skipor of Motorola CMRC and the donation of the composite substrates by Polyclad Laminates Inc.

APPENDIX A

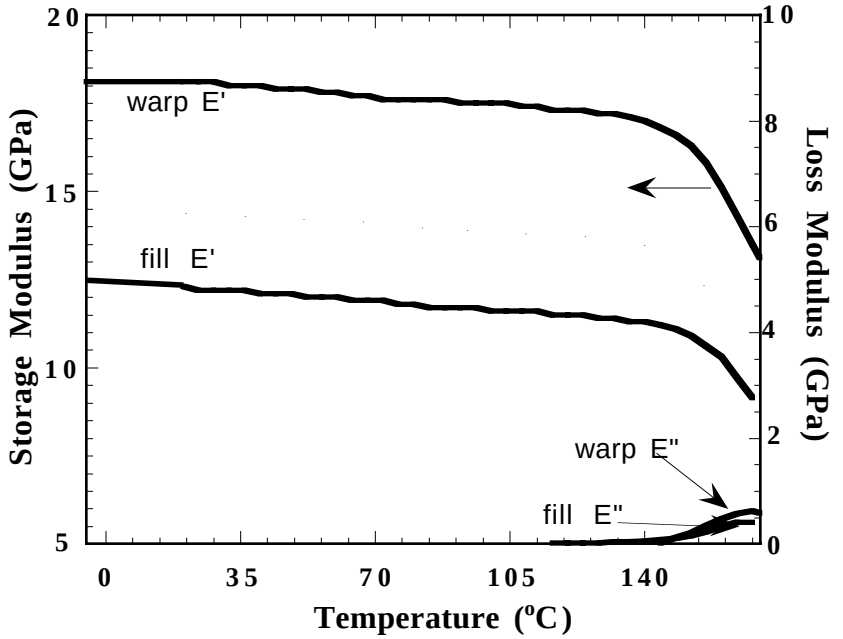

Fig. 11. Loss and storage modulus as a function of temperature for 1080 in the warp and fill directions.

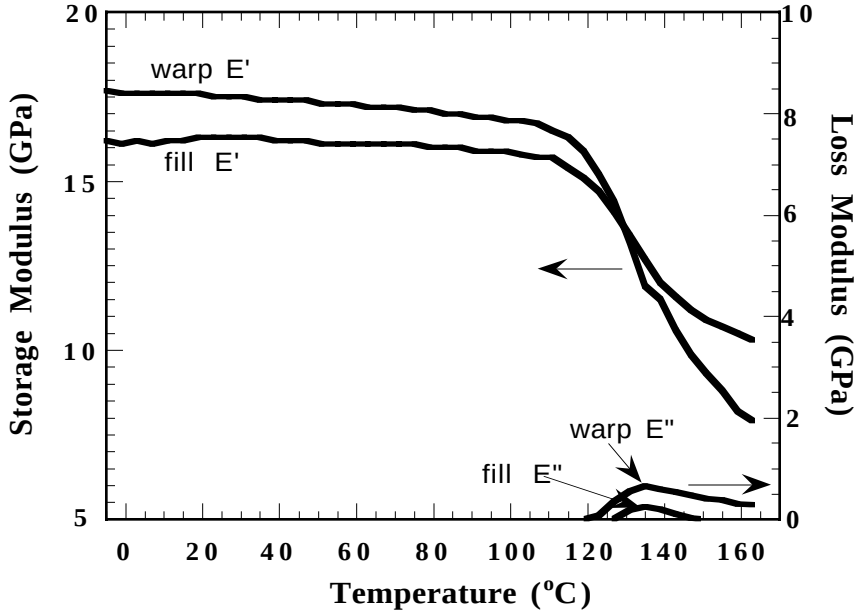

Fig. 12. Loss and storage modulus as a function of temperature for 2116 in the warp and fill directions.

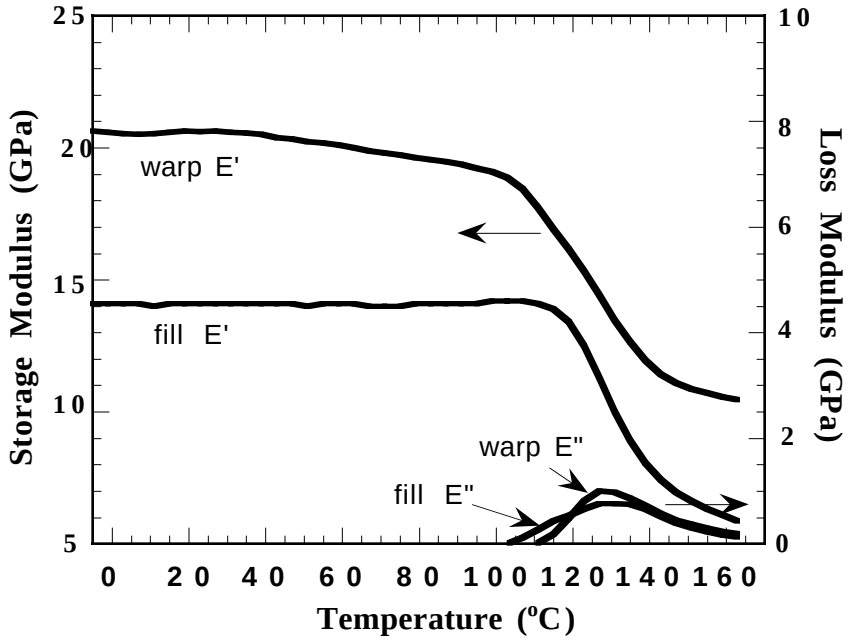

Fig. 13. Loss and storage modulus as a function of temperature for 2313 in the warp and fill directions.

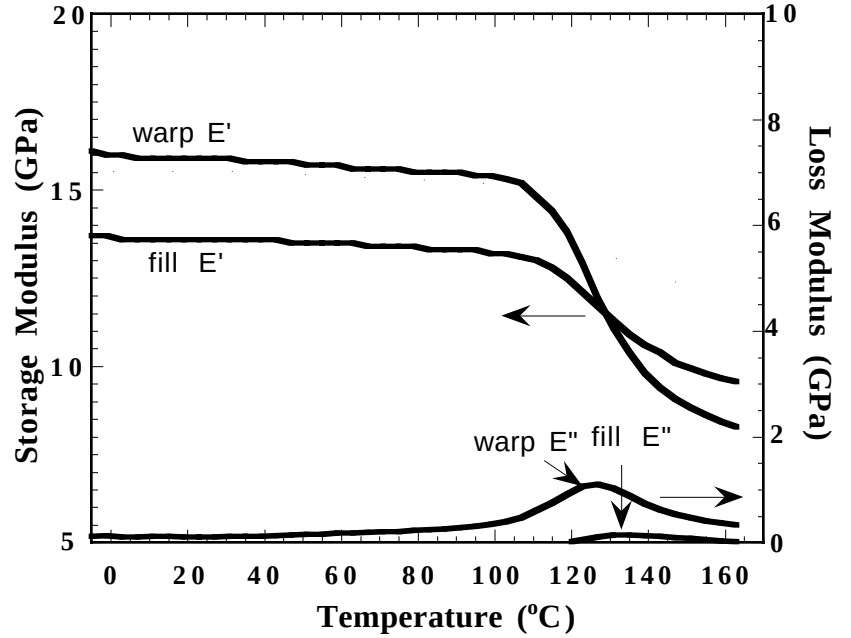

Fig. 14. Loss and storage modulus as a function of temperature for 3313 in the warp and fill directions.

APPENDIX B

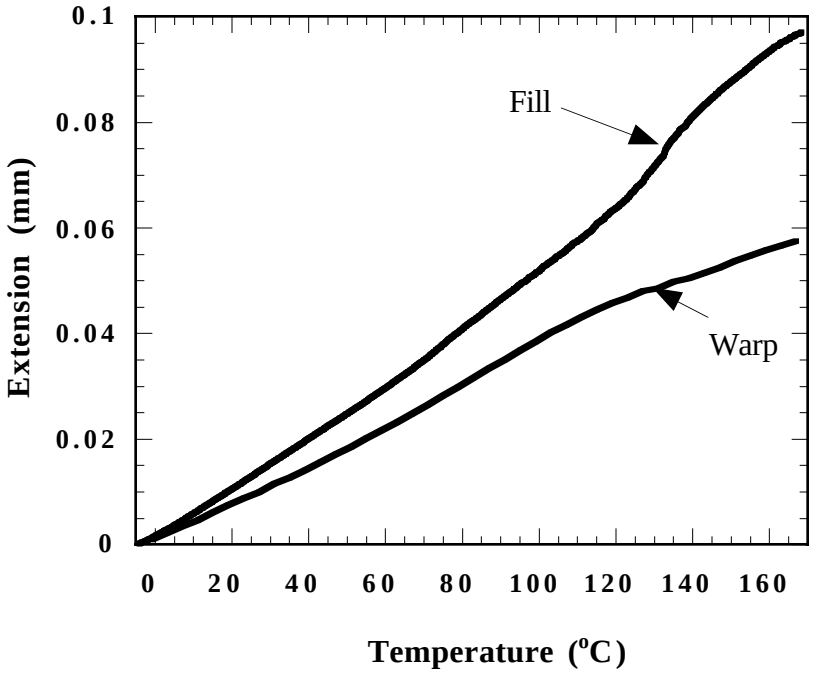

Fig. 15. Expansion as a function of temperature for 1080 in the warp and fill directions.

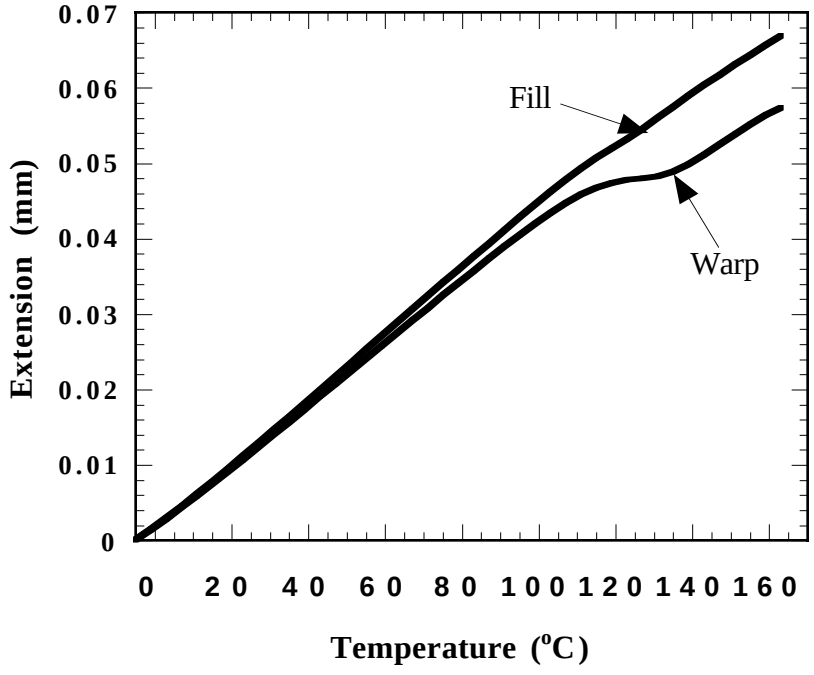

Fig. 16. Expansion as a function of temperature for 2116 in the warp and fill directions.

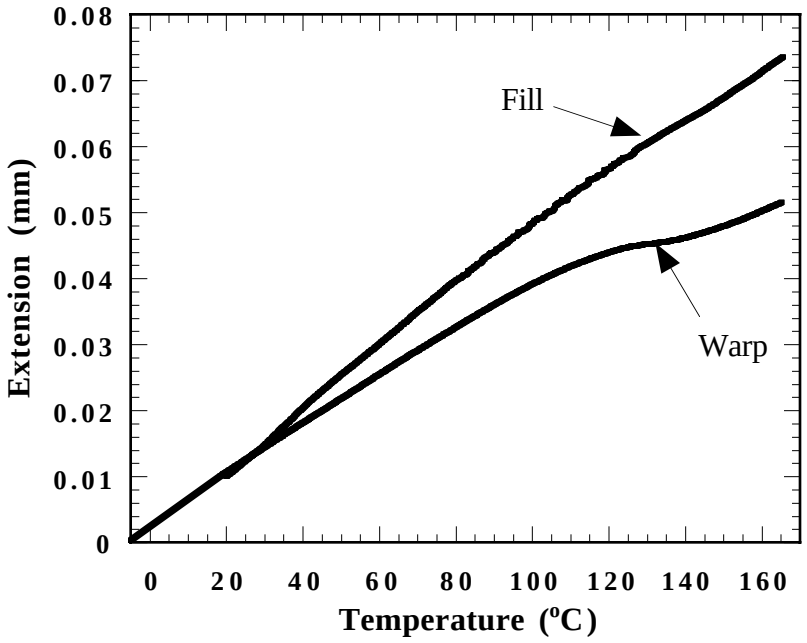

Fig. 17. Expansion as a function of temperature for 2313 in the warp and fill directions.

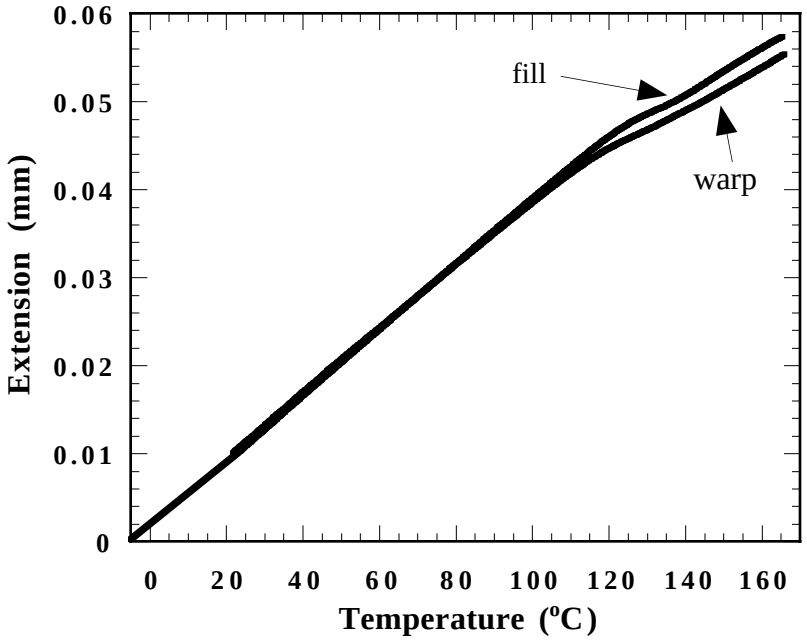

Fig. 18. Expansion as a function of temperature for 3313 in the warp and fill directions.

APPENDIX C

Through out this study, a Perkin-Elmer 7e Dynamic Mechanical Analyzer was used. In order to measure the CTEs of the sample substrates, the DMA was used in the TMA mode. During these experiments, the measured values of CTEs were consistently higher than values recorded by J. Yuan and L. A. Falanga (1992) for 7628 and 2116 substrates. Similarly, theoretical predictions by N. R. Sottos, J. M. Ockers, and M. Swindeman (1997) for the CTEs' of 2313 and 2116 substrates were lower than the experimentally measured CTEs. To minimize equipment expansion, Perkin-Elmer developed quartz probes with a very low CTE. In conjunction with the quartz probes, short steel clamps were used to rigidly hold samples in place. A review of the DMA equipment and process in conjunction with experimental measurements of the CTE of stainless steel standards indicated that the data acquisition and reduction program developed for the control of the DMA does not take the expansion of these steel grips into account when calculating sample expansions. This unaccounted expansion is comparable to the expansion of the 18 mm substrate samples resulting in the measured CTE being much higher that the expected values.

Comparisons between known CTEs of polymer standards and measured CTEs allowed for the development of a corrective equation for the thermal expansion of the test system. Knowing that the measured expansion has two components, the extension of the sample which is the desired unknown and the extension of the system, it was possible to determine the unwanted extension of the system. The measured change in length Δl_m is defined as the sum of the actual change of the composite sample plus that of the system,

$$\Delta l_m = \Delta l_c + \Delta l_s. \tag{2}$$

In terms of CTE (α),

$$\Delta l_m = \alpha_c \, l_c \, \Delta T_c + \alpha_s \, l_s \, \Delta T_s. \tag{3}$$

Solving for the CTE of the composite, with $\Delta T_c = \Delta T_s$, provides:

$$\alpha_c = \frac{\left(\Delta l_m / \Delta T\right) - CF}{l_c} \tag{4}$$

where

$$CF = \alpha_s \, l_s. \tag{5}$$

By inserting the known parameters of several material into the equation a value of $1.5x10^{-4}$ was found for CF. This correction calculation was used through out all of the TMA data reduction to measure glass/epoxy substrate coefficients of thermal expansion.

REFERENCES

Owens Corning, 1988, Glass Fiber Product Literature, IPC-EG-140.

Sottos, N.R., Ockers, J. M. and Swindeman, M. 1997, "Thermal Properties of Plain Composites for Multilayer Circuit Board Applications," To appear in *ASME Journal of Electronic Packaging.*

Wu, T. Y., Guo, Y. and Chen, W. T. 1993, "Thermomechanical strain characterization for printed wiring boards," In *IBM J. Res. Develop.*, Vol. 37 NO. 5, September, pp. 621-634.

Yuan , J. and Falanga, L. A. 1993, "The In-Plane Thermal Expansion of Glass Fabric Reinforced Epoxy Laminates," In *Journal of Reinforced Plastics and Composites*, Vol. 12, April, pp. 489-496.